QTAIM Analysis of the Bonding in Pyridyl- N-Heterocyclic Carbene Triruthenium carbonyl cluster: [Ru_3(μ-H)(μ-κ^3C_2,N-pyCH_2 ImMe) $(CO)_9$] (ImMe=3-methylimidazol-2- ylidene)

Muhsen Abood Muhsen Al-Ibadi
Department of Chemistry, College of Science, University of Kufa
muhsenabood@yahoo.com

Abstract

The bonding in the pyridyl N-Heterocyclic Carbene Triruthenium carbonyl cluster [Ru_3(μ-H)(μ-κ^3C_2,N-pyCH_2ImMe)$(CO)_9$] is explored using the Quantum Theory of Atoms-in-Molecules (QTAIM). The metal–metal and metal–ligand bond critical points properties are ρ(r), ∇^2ρ(r), H(r), G(r) and ellipticity. Also the bond delocalization indices δ(A, B), are correlated with the data from previous studies of the organometallic systems. These results have allowed a comparison between topological properties of different atom-atom interactions. At the core of triruthenium cluster, Ru_3H part, the topological data recognize the existence of a bond path in only two of the Ru(1)-Ru(2) and Ru(1)-Ru(3) edges, and there is no direct bond path has been found for the interaction between the hydride bridged Ru atoms, although a non-negligible delocalization index δ(Ru(2)...Ru(3)) has been obtained for this non-bonding interaction. A multicenter 4c–4e interaction is proposed to exist in the core part, Ru_3H. All topological parameters are calculated for the two existing Ru-C bonds between the ruthenium atoms and the pyridyl and NHC ligands are similar, and they confirm that these interactions are pure σ bond. The analysis of the topological parameters of the NHC and pyridyl ligands bonds confirm the existence of π-electron delocalization within the six-membered ring of pyridyl ligand and hindered π-electron delocalization within the five-membered ring of NHC ligand with some double-bond character in the interaction of the carbine C atom with the adjacent N atoms.

Kew words:- AIM bonding analysis Ruthenium clusters, Metal–Metal bonds, Metal–hydrogen and DFT calculations.

Introduction

The topological analysis of the electron density can be studied by the Bader quantum theory of Atoms in the Molecule (QTAIM).[1] This theory provides a powerful methodology for exploring various interactions in a molecular system and their ability to identify the bond between any two atoms in terms of bond critical points (BCPs). Within this framework, the link between bonding modes and topological properties of the electron density and its Laplacian has been fully achieved for light atom molecules.[2] However, such links are inadequate for heavier elements, such as the transition metals, because bonds to a transition metal display a different and much narrower spectrum of topological indexes.[3] In addition, the nature of the bonding interactions between transition metal atoms is not completely understood yet and much argument is still occurring on its actual presence, role and mechanism. A few topological studies on cluster compounds with three or more metal–metal interactions between transition metal atoms have appeared recently.[4] Therefore, more QTAIM studies on this class of complexes are desirable in order to shed additional light on the relationship between metal-metal bonds and the topology of their associated electron density.

In recent years, the interest of the chemical community in the NHC-derived chemistry of transition-metal cluster and their catalytic properties has led many researchers to include polydentate NHCs ligands in their investigations.[5] Also, chemists have dedicated many efforts to investigate the coordination chemistry of NHCs ligands. These investigations have shown that, among other characteristic properties, NHC ligand has shown the ability to bind more strongly to metal atoms than most classical ligands, such as phosphenes, thus preventing dissociation equilibria.[6] In addition, NHCs are highly electron donating ligand (strong σ-donor ligand) and bulky[7] with a high steric hindrance. These features have led to important breakthroughs in homogeneous catalysis.[8]

A few of AIM theoretical analysis of bonding NHC-metal complexes have been published to date.[9-11] For instance, Scherer et al.[9] and Tafipolsky et al.[10] have re-examined the charge-density in Cr-NHC, using QTAIM. Both studies have concluded that π-electron delocalisation within the five-membered ring is not completely but slightly hindered instead. A similar conclusion was reached by Cabeza and co-workers[11] from the investigation of NHC-diydride triruthenium cluster $[Ru_3(\mu\text{-}H)_2\text{-}(\mu^3\text{-}MeImCH)(CO)_9]$ using the QTAIM analysis. Moreover, they found only bond path between unbridged ruthenium atoms and the Ru–NHC interaction is pure σ-bonds.

This paper reports the results of a QTAIM topological analysis of the electron density in the pyridyl-NHC Triruthenium cluster $[Ru_3(\mu\text{-}H)(\mu\text{-}\kappa^3C_2,N\text{-}pyCH_2ImMe)(CO)_9]$, Figure 1, have previously reported by Cabeza group,[12] to obtain a deeper insight into the nature of the chemical bonding.

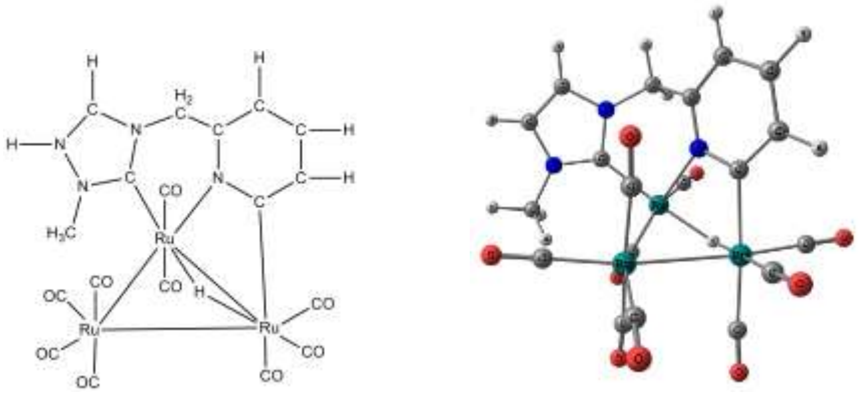

(a) (b)

Figure 1. (a) schematic structure and (b) geometry optimization structure of $[Ru_3(\mu\text{-}H)(\mu\text{-}\kappa^3C_2,N\text{-}pyCH_2ImMe)(CO)_9]$.

This cluster has been chosen due to the following reasons: firstly, there was no previous QTAIM studies on pyridyl NHC Triruthenium cluster has been hitherto reported. Secondly, this particular cluster contains two unbridged Ru-Ru bonds and one hydride bridged Ru-Ru edge with two types of Ru-C bonds (Figure 1). This allows interesting comparisons between the topological properties of related but different atom–atom interactions, within the same molecule, and Ru-C_{NHC} versus Ru-$C_{pyridyl}$ interactions.

Computational Methods

The X-ray diffraction structure of pyridyl-NHC triruthenium cluster $[Ru_3(\mu\text{-}H)(\mu\text{-}\kappa^3C_2,N\text{-}pyCH_2ImMe)(CO)_9]$ was used as a starting points for geometry optimization, which was performed with the GAUSSIAN09[13] package at the DFT level of theory, using PBE1PBE[14] functional. For this case, all electron 6-31G(d, p)[15] basis set were employed for H, C, N and O atoms. The SDD[16] effective core potential (ECP) basis set was used for Ru atoms. An extra set of f-polarisation functions was added to the Ru ($\alpha f = 1.235$).[17] The AIM results described in this work correspond to calculations performed with the PBE1PBE/WTBS[18]/6-31G(d, P) model. These calculations included both local and integral topological properties were carried out with the AIM2000 program.[19]

Results and Discussion

Topological Analysis of the Electron Density:

The main feature of atoms in molecules (AIM) theory of Bader,[1] with the AIM2000 program package, is that the topology or the surface features of electron density contains very useful information about the bonding situation. In addition, this topology has proved to be an appropriate tool for studying a wide spectrum of metal–metal and metal–ligand interactions. Specifically, the topology of the electron density $\rho(r)$ at the critical points, i.e. the points in space at which the gradient of the density vanishes ($\nabla\rho$ (r) = 0), carries important information about the covalency and multiplicity of the bond. A critical point that is characterised by two negative curvatures (maximum) and one positive curvature (minimum), labelled as (3, -1), is referred to as a bond critical point (BCP) and is considered to be indicative of the presence of a bonding interaction between two atoms. A ring critical point (RCP), in contrast, has one negative curvature and two positive curvatures, and is labelled as (3, +1). Some structures necessarily contain other critical point of the density: the (3, +3) is produced inside a cage of at least four bonded atoms (cage critical point, CCP). From the QTAIM perspective, a chemical bond is simply the line of maximum electron density (bond path, BP) between two atoms and intersects an interatomic surface at the bond critical point. Based on this definitions, the existence of BP and BCP is considered to be indicative of the presence of chemical bond between two atoms or not.

First, we analyze the existence of bonding in the pyridyl NHC triruthenium cluster by performing the QTAIM analysis. The molecular graph is shown in Figure 2.

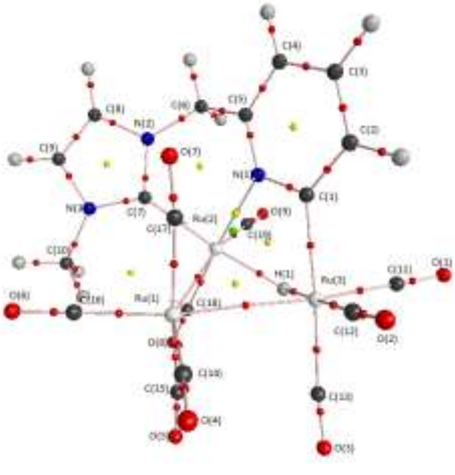

Figure 2. Molecular graph of the pyridyl NHC triruthenium cluster, showing the bond paths (gray lines) with the bond (small red circles between two atoms) and ring (yellow circles) critical points.

From the molecular graph, one can easily observe the bonds and ring critical points, together with the bond paths that connect the bonded atoms through their corresponding bond critical points. The bcp's and bp's for the Ru-Ru, Ru-C, Ru-H, C-O, C-N, C-C, and C-H bonds were clearly found. Interestingly, in the Ru_3H, the existence of bcps and bps were only in the edges that are not bridged by the hydride ligands, Ru(1)-Ru(2) and Ru(1)-Ru(3) bonds. On the other hand, a bcp's and bp's are not observed between the hydride-bridge ruthenium atoms, Ru(2) and Ru(3), so that, we can presume no direct Ru-Ru bonding is present. This loss of a metal-metal bond path when bridged by the hydride ligands[11] has been also observed for other bridging ligands such as CO,[20, 4a] borylenes,[21] alkynes[22] and alkylidynes.[23] Five rcp's were clearly observed, corresponding to the C(7)-N(2)-C(8)-C(9)-N(3), Ru(2)-N(1)-C(1)-Ru(3)-H(1), Ru(1)-Ru(2)-H(1)-Ru(3), Ru(2)-N(1)-C(5)-C(6)-N(2)-C(7) and C(1)-C(2)-C(3)-C(4)-C(5)-N(1) rings.

A gradient trajectory map of the total electron density in the Ru(1)-Ru(2)-Ru(3) plane with the atomic basins are depicted in Figure 3. It shows that the bps and bcps between Ru(1), Ru(2) and Ru(3) together with the atomic basins for these and other atoms located in the same plane. The atomic basins, bcp's and bp's of two CO ligands, located in the same plane, which are also visible in the plot. A projection for the position of the H(1) hydride ligand on this plane is also shown.

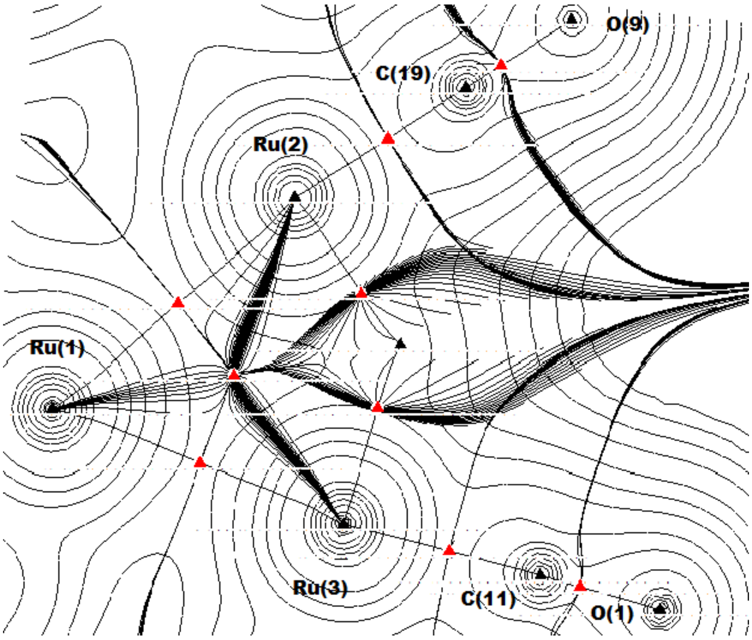

Figure 3. Gradient trajectories mapped on a total electron density plot in the Ru(1)-Ru(2)-Ru(3) plane, showing the atomic basins, bp's and bcp's.

A gradient trajectory map of the total electron density in the plane spanned by the pyridyl ligand, showing the bp's, bcp's and rcp associated with this ligand, is depicted in Figure 4. The bcp's and bp's, found between Ru(2) and Ru(3) with the pyridyl ligand N(1) and C(1) atoms respectively, located in this plane can also be observed. The C(6) is also located on the pyridyl ligand plane, and it is bonded to C(5) in pyridyl group.

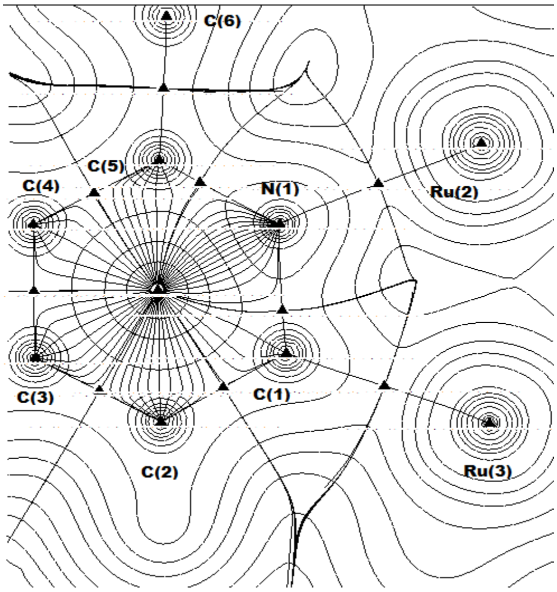

Figure 4 Gradient trajectories mapped on a total electron density plot in the pridyl ligand plane, showing the atom basins, bp's , bcp's and rcp.

Figure 5 displays a gradient trajectory map of the total electron density in the plane spanned by the NHC ligand showing the bp's, bcp's and rcp associated with this ligand. Both bcp and bp are found between Ru(2) with the NHC ligand C(7) atom. In this figure, the C(3) and C(6) are also located on the NHC ligand plane, and they are bonded to N(3) and N(2) respectively, in NHC group.

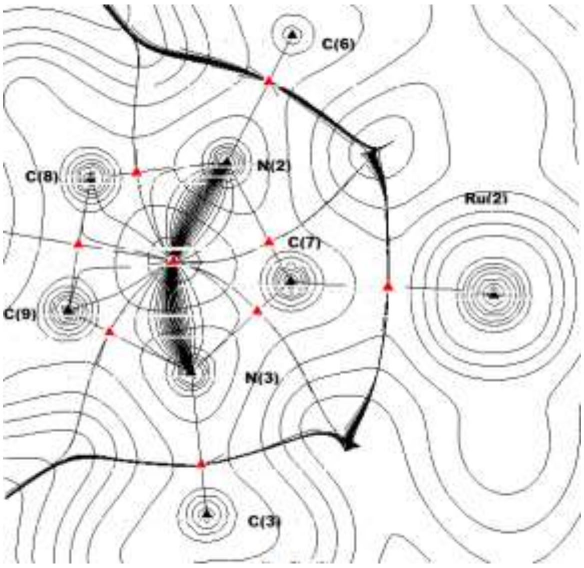

Figure 5. Gradient trajectories mapped on a total electron density plot in the NHC ligand plane, showing the atom basins, , bp's , bcp's and rcp.

Atoms in Molecules Analysis

In Bader's topological QTAIM analysis, the nature of bonding in molecules is analyzed in terms of the properties of electron density and its derivatives. Among these derivatives, the Laplacian , $\nabla^2\rho(r)$, as a second derivative of the electron density, which is a useful indicator for the nature of the chemical bonding, which links between two important quantities, the kinetic energy density $G(r)$ (everywhere positive, $G(r) \geq 0$) and the potential energy density ***V(r)*** (everywhere negative, $V(r) \leq 0$), in a local virial theorem:[1]

$$\frac{1}{4} \nabla^2 \rho(r) = 2G(r) + V(r) \qquad (1)$$

The magnitude and the sign of Laplacian at a BCP are determined by which energy is in excess over the viral average of 2:1 of kinetics to potential energy. In shared-electron (covalent) interactions, with negative value of $\nabla^2\rho(r)$, the potential energy density is dominant and the electron density is concentrated along the bond path linking the bonded atoms. Conversely, in closed-shell (electrostatic) interactions the electron density is expanded relating to its average distribution. Therefore, $\nabla^2\rho(r)$ is a positive value at the BCP and the kinetic energy density is dominant. Apart from this, the electronic energy density, *H(r)*, as :

$$H(r) = G(r) + V(r) \qquad (2)$$

This equation can be used to compare the kinetic and potential energy densities on an equal footing. For all interactions with significant sharing of electrons, *H(r)* is negative at the bcp, and its absolute value reflects covalent character of the interaction or dative nature.[1] On the other hand, the ellipticity $\varepsilon(r)$ at bcp is a measure of π-character of the bonding: values close to zero indicate a cylindrically symmetric bond, while deviations away from zero indicate increasing π-character. For reference, the ellipticity values for ethane and ethene are 0.0 and ~ 0.3, respectively.[2, 24]

Table 1. Selected topological properties at the critical points for triruthenium cluster: electron density, Laplacian, total energy density ratio, kinetic energy density ratio and ellipticity.

Bond	ρ_b(eÅ^{-3})	$\nabla^2\rho_b$(eÅ^{-5})	H_b(he^{-1})	G_b(he^{-1})	ε_b
Ru(1)-Ru(2)	0.340	0.492	-0.051	0.174	0.054
Ru(1)-Ru(3)	0.350	0.512	-0.051	0.180	0.035
Ru-H (ave)	0.805	1.970	-0.247	0.740	0.044
Ru-CO (ave)	1.490	5.210	-0.650	1.960	0.148
Ru(3)-C(1)	1.140	2.400	-0.420	1.020	0.076
Ru(2)-N(1)	0.889	4.200	-0.126	1.180	0.057
Ru(2)-C(7)	1.190	3.160	-0.430	1.230	0.054
C-O (ave)	4.540	11.610	-7.430	10.340	0.002
N(3)-C(10)$_{\text{methyl}}$	2.600	-6.640	-3.640	1.981	0.025
Pridyl-ligand					
N(1)-C(1)	3.230	-5.760	-5.310	3.860	0.047
C(1)-C(2)	3.080	-8.400	-3.070	0.964	0.166
C(2)-C(3)	3.150	-8.760	-3.227	1.030	0.203
C(3)-C(4)	3.110	-8.560	-3.127	0.983	0.185
C(4)-C(5)	3.170	-8.800	-3.270	1.060	0.252
C(5)-N(1)	3.350	-0.804	-5.530	3.510	0.141
C(5)-C(6)	2.620	-6.560	-2.220	0.580	0.056
NHC-ligand					
C(7)-N(2)	3.150	-5.920	-5.140	3.660	0.082
C(7)-N(3)	3.170	-6.160	-5.180	3.630	0.101
C(8)-N(2)	3.010	-6.282	-4.760	3.180	0.165
C(9)-N(3)	3.030	-6.600	-4.790	3.140	0.165
C(8)-C(9)	3.370	-9.688	-3.690	1.260	0.405
C(6)-N(2)	2.620	-7.320	-3.480	1.650	0.048

Ru$_3$H Interactions

In the framework of QTAIM we calculated some topological properties of the coordination bonded interactions in the triruthenium cluster molecule (Table 1). Here, the Ru(1)-Ru(2) and Ru(1)-Ru(3) interactions are typical open-shell metal-metal interactions, intermediate between pure covalent and pure ionic bonds between non metal atoms, with the value of the electron density (0.340 and 0.350 e Å^{-3} respectively, at the bcps), the positive but small value of the Laplacian (0.492 and 0.512 eÅ^{-5}), the positive but less than unity value of G_b (0.174 and 0.180 he^{-1}) and small value of ε_b (0.054 and 0.035). These values are comparable to those reported for Ru-Ru bonds in [Ru$_2$-(formamidinate)$_4$],[25] [Ru$_3$(CO)$_{12}$][26] and [Ru$_3$(μ-H)$_2$(μ^3-MeImCH)(CO)$_9$].[11] For instance, in the latter compound, the electron density ρ_b, laplacian $\nabla^2\rho_b$, kinetic energy G_b and ellipticity ε_b values for unabridged Ru-Ru bond are 0.292 eÅ^{-3}, 0.803 eÅ^{-5}, 0.463 he^{-1} and 0.036 respectively. It is interesting to note that there is no bcp's or direct bp's were found between the hydride-bridged Ru(2) and Ru(3) interaction. For the Ru-H interactions, an average value of 0.805 eÅ^{-3} and 1.970 eÅ^{-5} for the electron density and Laplacian indicate that the strength of these bonds is comparable to that of pure covalent single bonds between nonmetal atoms.[4a] Additionally, the ellipticity ε(Ru-H) for ruthenium cluster 1 (0.044) is comparable to ε(Ru-H) for [Ru$_3$(μ-H)$_2$(μ^3-MeImCH)(CO)$_9$] (0.086).[11] The very low ellipticities of these bonds are related to the bond symmetry.

The Ru-Ru and Ru-H interactions in the Ru$_3$H part of the cluster may also be analyzed by looking at the Laplacian of the electron density in the Ru(1)-Ru(2)-H(1)-Ru(3) (Figure 6) plane of the molecule. Valence shell charge concentration (VSCC) of bridging hydrogen H(1) atom is polarized toward the midpoint of the Ru(2)-Ru(3) edge. These polarizations are small, giving slightly more positive values for the Laplacian in the two Ru-H bcp's (an avarage 1.970 eÅ^{-5}) than those expected in the absence of such polarization.

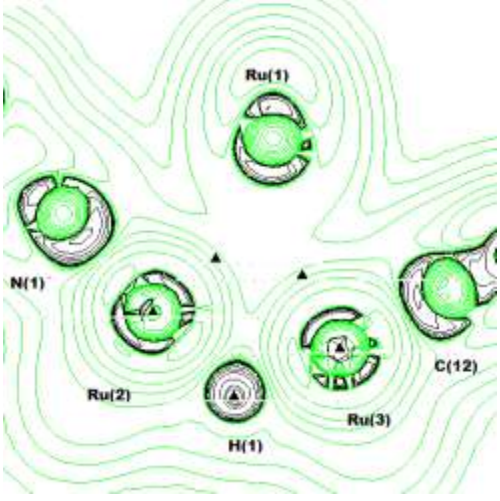

Figure 6. Laplacian map of the electron density in the Ru(1)-Ru(2)-H(1)-Ru(3) plane of triruthenium cluster.

This graph also shows that the VSCCs for both bridging N(1) and carbonyl C(12) atoms distorted towards their bonded Ru atoms. The former has a similar situation to that previously observed for the C atoms coordinated to NHC ligand bridging two Ru atoms.[11]

Delocalization Indices.

The integrated topological properties are more useful than the local topological properties for characterizing metal-metal bonds.[25, 27] In this sense, the delocalization index δ(A-B), which is an integral property, is one of the most powerful tools, provides a measure of the Fermi correlation shared (and hence electrons shared) between two atomic basins A and B.[28] Regardless of whether they are formally bonded, this index can be computed for any pair of atoms. According to AIM, the delocalization index provides directly the number of electron pairs shared by atoms A and B but does not have any direct relationship to bond order.[29] Table 2 gives the delocalization indices for specific atomic δ(A, B) interactions in 1.

Table 2: Delocalization Indices *δ(A, B)* for Compound 1

atom pairs (A, B)	δ(A, B)	atom pairs (A, B)	δ(A, B)
Ru(1)-Ru(3)	0.406	C(7)-N(2)	0.967
Ru(1)-Ru(2)	0.399	C(7)-N(3)	0.974
Ru-H (ave)	0.468	N(2)-C(8)	0.961
Ru(3)-C(1)	0.755	N(3)-C(9)	0.964
Ru(2)-N(1)	0.544	C(8)-C(9)	1.352
Ru(2)-C(7)	0.815	N(3)-C(10)	0.819
Ru-CO (ave)	1.101	Ru(2)...Ru(3)	0.199
C-O (ave)	1.494	Ru…$\mathrm{O_{CO}}$ (ave)	0.187
N(1)-C(1)	1.076	Ru(2)...N(2)	0.064
C(1)-C(2)	1.159	Ru(2)...N(3)	0.058
C(2)-C(3)	1.276	Ru(2)...C(1)	0.045
C(3)-C(4)	1.194	Ru(2)...C(5)	0.024
C(4)-C(5)	1.186	Ru(3)...C(2)	0.043
C(5)-C(6)	0.861	Ru(3)...N(1)	0.076
C(5)-N(1)	1.047	Ru(1)…N(2)	0.005
C(6)-N(2)	0.81	Ru(1)…N(3)	0.011

The delocalization indices calculated for the two unbridged Ru-Ru bonds, the Ru(1)-Ru(2) and Ru(1)-Ru(3) bonds, are smaller and less than 0.5; nevertheless, these values are in line with the few cases reported previously for unbridged metal-metal bonds, such as the Ru-Ru bond (0.458) in $[\mathrm{Ru_3(\mu\text{-}H)_2\text{-}(\mu^3\text{-}MeImCH)(CO)_9}]$[11], the Os-Os bonds (in the range 0.350-0.461) in $[\mathrm{Os_3(CO)_{12}}]$, $[\mathrm{Os_3(\mu\text{-}H)(\mu\text{-}Cl)(CO)_{10}}]$, $[\mathrm{Os_3(\mu\text{-}H)(\mu\text{-}OH)(CO)_{10}}]$ and $[\mathrm{Os_3(\mu\text{-}H)_2(CO)_{10}}]$ [30], the Fe-Fe bond (an average 0.398) in $[\mathrm{Fe_3(\mu\text{-}H)(\mu\text{-}COMe)(CO)_{10}}]$[31], and in line with the few cases reported to date for other M-M interaction.[32] In contrast, the nonbonding interaction, hydride-bridged Ru(2)...Ru(3), has, as expected, low value for their delocalization indices (0.199). This value is comparable in magnitude to hydride-bridged M...M interactions, for instance, (between 0.169 and 0.246) for Ru...Ru interactions of $[\mathrm{Ru_3(\mu\text{-}H)_2\text{-}(\mu^3\text{-}MeImCH)(CO)_9}]$[11], (0.270) for Os...Os interaction of $[\mathrm{Os_3(\mu\text{-}H)_2(CO)_{10}}]$[30] and (0.208) for Fe...Fe interaction of $\mathrm{Fe_3(\mu\text{-}H)(\mu\text{-}COMe)(CO)_{10}}$,[31] or even greater than other values found for ligand-bridged M...M interactions in several organometallic compounds.[27, 4a, 33] On the other hand, the delocalization indices of the Ru(2)...Ru(3) interaction is comparable to those previously reported for unbridged metal-metal interaction, for example, the Co-Co of $[\mathrm{Co_2(CO)_8}]$ (0.46).[34] Therefore, the fact that the bridged Ru-Ru interaction has smaller delocalization index compared with the unbridged Ru-Ru interaction could provide some evidence for bridge participation in bonding.

An average value of 0.468 for the delocalization index of the Ru-H interactions of 1 (Table 2) is marginally lower than δ(Ru-H) interactions for $[Ru_3(\mu\text{-}H)_2(\mu^3\text{-}MeImCH)(CO)_9]$[11] (0.474) and in line with few cases reported for M-H interactions.[32] Rather interestingly, the calculated delocalization index values for the Ru(2)-H(1) and Ru(3)-H(1) interactions suggest that there are about half an electron pair shared in each of the two Ru-H bonds , just as in the Ru(1)-Ru(2) and Ru(1)-Ru(3) bonds, although the topology of both kinds of bonds is quite different, as reflected by their local topological parameters calculated in Table 1.

Then, by summarizing all these features, it is interesting to note that the sum of all of the delocalization indices involving the four δ(A-B) values for the bonding interactions and the one δ(Ru...Ru) value for the nonbonding interactions in the Ru(1)-Ru(2)-H(1)-Ru(3) plane, is roughly constant at ～2 electron pairs. It can be concluded that there exists a multicenter (4c-4e) interaction in the core part, Ru_3H, of compound 1.

Ru-CO Interactions

For the Ru-CO interactions of triruthenium cluster 1, the mean value given in table 1 for the $\rho_{(b)}$ value is close to 1.490 $Åe^{-3}$, higher than those of metal-metal bonds but lower than those of pure covalent single bonds between nonmetal atoms, a large positive value (5.210 $Åe^{-5}$) of $\nabla^2\rho_{(b)}$, a value of around 1.960 he^{-1} for G_b, and a small negative value for $H_{(b)}$ (-0.650 he^{-1}), are in line with those reported in the literature for metal-CO bonds.[32, 35-39]

In addition, the delocalization index value of δ(Ru-C), for the Ru-carbonyl bonds may be inferred it to measure a formal bond order of 1, but unfortunately, it is difficult to detect the π-back-donation from the Ru to the CO ligand because the cylindrical symmetry of the density along the Ru-CO bond path hides any trace of preferential accumulation planes.

Instead of, the value of $\delta(M...O_{CO})$ is also a reasonable sign of the presence or absence of π-back-bonding in M-CO bonds because the π-back-donation involves significant $M...O_{CO}$ interaction. The reader is directed to review that cover this topic in more detail.[4a] Hence, delocalization indexes for the $\delta(M...O_{CO})$ interactions were calculated to establish the presence or absence of any kind of π-bonding in the Ru-CO bond as shown in table 2. The $\delta(Ru...O_{CO})$ values (0.187 on average) are nearly equal to those found for the delocalization indexes of the $Ru...O_{CO}$ for $[Ru_3(\mu\text{-}H)_2\text{-}(\mu^3\text{-}MeImCH)(CO)_9]$[11] (0.202) and within the range (0.15 to 0.25) of $\delta(M...O_{CO})$ for Co, Fe, and Ni carbonyl complexes (in which π-bonding is obviously possible), indicating the presence of π-back-donation. In comparison, $\delta(Cu...O_{CO})$ = 0.09 for $[Cu(CO)_2]^+$ and $\delta(B...O_{CO})$ = 0.04 for H_3BCO, in which no π-back-donation exists. [4a]

These results are also confirmed by the topological indexes of the C-O bonds of 1 (Table 1), which are consistent with a weakening of the C-O bonding (smaller density, Laplacian, |Hb/Fb|, and Gb/Fb) in comparison with that of free CO or H_3BCO.

Ru-C_{NHC} and Ru-C_{Pyr}, N_{Pyr} interactions

In this context, we considered it interesting to compare Ru-C_{NHC} with Ru-C_{pyr} bond, on the one hand, and the former with Ru-N_{pyr} bond, on the other hand. The values of the topological indexes for the Ru(2) atom and the carbine C(7) atom of NHC ligand, included in table 1, are similar to these found for almost equivalent bond between Ru atoms and the C-Pyridyl ligand, Ru(3)-C(1), which involve the sp^3-hybridized C atom. These values are comparable to those previously found, from both experimental and theoretical electron densities, such as the M-$C_{carbene}$ bond in $[Ru_3(\mu\text{-}H)_2(\mu^3\text{-}MeImCH)(CO)_9]$,[11] $Fe_3(\mu\text{-}H)(\mu\text{-}COMe)(CO)_{10}$,[31] $[Co_2(\mu\text{-}\eta^1\text{-}C_4O_2H_2)(\mu\text{-}CO)(CO)_6]$,[39] $[Cr\{C\text{-}(NH_2)CH_3\}(CO)_5]$[38] and $[Cr(Me_2Im)(CO)_5]$.[9-10] For instance, the ellipticity at the bcp of the Ru-$C_{carbene}$ bond of $[Ru_3(\mu\text{-}H)_2(\mu^3\text{-}MeImCH)(CO)_9]$ and Cr-Ccarbene bond of $[Cr(Me_2Im)(CO)_5]$, which has the same NHC ligand as ruthenium cluster, which was found to be between 0.04-0.08 (calculated) and 0.08 (experimental), very close to the value found for ruthenium cluster 1 (0.054 and 0.076). A similar feature has been found for the Laplacian (between 6.0-6.7 and 7.1 e Å^{-5} for the Cr and Ru complexes respectively, vs 2.8 e Å^{-5} on average for ruthenium cluster 1), whereas $\rho_{(b)}$ (0.52 and 0.74 vs 1.140-1.190 Å e^{-3}) are not so close. These values suggest that the strength of these bonds is comparable to those of pure covalent single bonds between non metal atoms.[4a] The delocalization indexes computed for the two Ru-C_{NHC} and Ru-C_{pyr} intractions in 1 are very similar, 0.815 for Ru(2)-C(7) and 0.755 for Ru(3)-C(1), and their values indicate that about 0.8 electron pair is shared between each pair of bonded atoms, are also very similar to those calculated for Ru-C_{NHC} bonds in $[Ru_3(\mu\text{-}H)_2(\mu^3\text{-}MeImCH)(CO)_9]$.[11] As expected, the Figure 6 shows that the VSCCs of C(1) and C(7) atoms are distorted toward the ruthenium atoms to which they are attached.

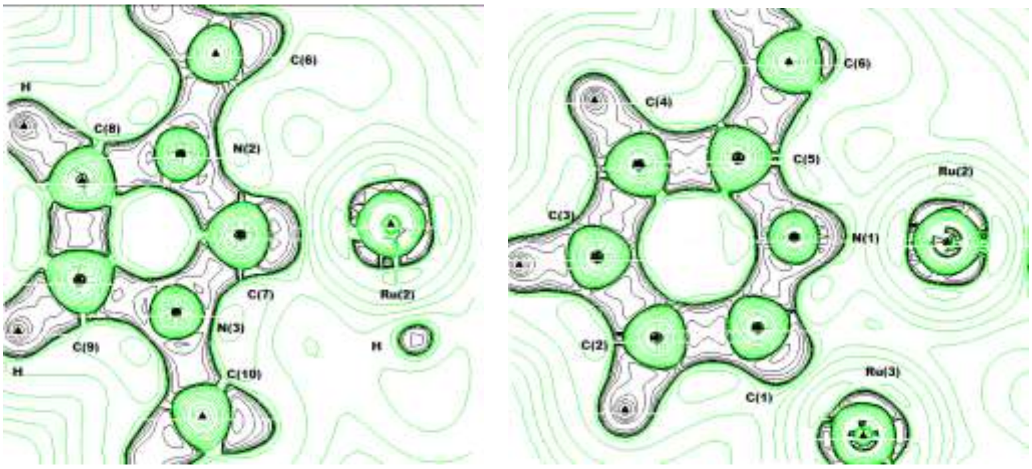

(a) (b)

Figure 7. Laplacian of the electron density in the (a) NHC ligand (b) Pridyl ligand planes

Regarding to the bonds between Ru atoms and the N-Pyridyl ligand, Ru(2)-N(1), it is quite interesting to compare with Ru(3)-C(1). The former have smaller value of electron density, high values of the Laplacian and slightly smaller ellipticity as depicted in Table 1. These results indicate that the Ru(3)-C(1) has slightly greater π-character than the Ru(2)-N(1) bond.

As discussed above, the value of $\delta(M...O_{CO})$ is a reasonable sign of π-bonding in M-CO bonds, the delocalization indexes for the Ru(2)...N(2, 3) , Ru(2)...C(1, 5) and Ru(3)...N(1), C(2) interactions were calculated, Table 2, in an attempt to establish the presence or absence of any kind of π-bonding in the Ru(2)-C(7), Ru(2)-N(1) and Ru(3)-C(1) bonds, respectively. These values are very small and nearly equal to those found for the delocalization indexes of the Ru(1)...N(1, 2), C(1, 2, 5) interactions, for which no π-bonding exists. Therefore, the pyridyl and NHC ligands of complex 1 behave as a pure σ-donor.

C-C and C-N Interactions within the NHC and Pyridyl Ligands

The topological properties of the bonding between the atoms of the NHC and pyridyl ligands are presented in Tables 1 and may be graphically visualized in Figures 4, 5 and 7. The gradient trajectory maps show the bcp's and bp's found between the atoms of the NHC and pyridyl ligands as well as their atomic basins. As expected for polar bonds, with the only exception of the C-C bonds, the positions of the bcp's are not symmetrical but shifted toward the less electronegative atom.

The topological parameters values of the NHC ligand bonds are typical for covalent bonds between non-metal atoms with some degree of delocalization.[2, 40] In this context, we considered it quite interesting to compare the topological parameters of N(2)-C(7) and N(3)-C(7) bonds with those of the N(2)-C(8) and N(3)-C(9) bonds. The formers have high values of the electron density at the bcp, moderate values of the laplacian and smaller value of ellipticity. These results indicate that the N(2)-C(8) and N(3)-C(9) bonds have a slightly greater character of double bonds than the N(2)-C(7) and N(3)-C(7) bonds. These facts support the proposal that the unsaturation of the carbene C(7) atom of an NHC ligand is alleviated by π-donation of electron density from the filled p-π orbitals of the N(2) and N(3) atoms to the empty p-π orbital of the C(7) carbene atom.[6b] The highest electron density value (3.370 $Åe^{-3}$) for the NHC ligand of ruthenium cluster belongs to the C(8)-C(9) bond, which also possesses the highest value of ellipticity (0.405) and the most negative value for the Laplacian (-9.688 $Åe^{-5}$) at bond critical points, values that are consistent with the presence of double bond character with a certain degree of delocalization within the NHC five-membered ring. On the contrary, the topological properties of the N(2)-C(6) bond are prototypical for a formal single covalent bond.

Regarding the pyridyl ligand, the highest value of electron density, the most negative value for the Laplacian and ellipticity for C-C and C-N bonds is consistent with a formal double bond with a certain degree of delocalization.

Conclusions

A number of topological parameters, local and integral, of the electron density for the pyridyl N-Heterocyclic carbene triruthenium carbonyl cluster $[Ru_3(\mu\text{-}H)(\mu\text{-}\kappa^3C_2,N\text{-}pyCH_2ImMe)(CO)_9]$ have been calculated under the prospective of the QTAIM approach. Although these results recognize the existence of a bond path only in the edge that is not bridged by the hydride ligands i.e., Ru(1)-Ru(2) and Ru(1)-Ru(3), the topological properties of the hydride-bridged Ru-Ru edges suggest a delocalized kind of interaction in the central part of the molecule. Thus, a mlticenter (4c-4e) interaction involving the Ru_3H core of the molecule here proposed. The topological parameters calculated for the two existing Ru-C bonds between ruthenium atoms with pyridyl and NHC ligands are similar, and they confirm that these interactions are pure σ-bonds.

Analysis of the topological parameters in the NHC ligand is consistent with the presence of some π-electron delocalization within the five-membered ring as well as the existence of some double-bond character in the interaction of the carbene C atom with the adjacent N atoms. Thus, the AIM theory supports the proposal that the unsaturation of the carbene C atom of NHC ligand is alleviated by donation of electron density from the filled p-π orbitals of the N atoms to the empty p-π orbital of the carbene carbon. Also, the calculated topological parameters of the pyridyl ligand bonds confirm the existence of π-electron delocalization within the six-membered ring. Along this work, it has been proven that the QTAIM provides very accurate tool to describe the chemical bonding, unambiguously the existence or absence of bonding between two atomic centers, as also highlighted by other researchers.[41] In addition, to the best of our knowledge, no previous studies dealing with the bonding interaction between pyridyl, NHC ligands and triruthenium cluster have appeared in the literature. This work contributes to shed more light on these areas.

5. References

[1] (a) R. F. W. Bader, *Atoms in Molecules a Quantum Theory*, Oxford University Press, Oxford, **1990**. (b) R. F. W. Bader, *J. phys. Chem. A* **1998**, 102, 7314.

[2] R. F. W. Bader, *J. Phys. Chem.*, **1998**, A102, 731.

[3] (a) J. F. Van der Maelen, J. Ruiz, S. García-Granda, *J. Theor. Comput. Chem.*, **2005**, 4, 823. (b) J. F. Van der Maelen, E. Gutiérrez-Puebla, A. Monge, S. García-Granda, I. Resa, E. Carmona, M. T. Fernández-Díaz, G. J. McIntyre, P. Pattison, H. -P. Weber, *Acta Crystallogr.*, **2007**, B 63, 862. (c) L. J. Farrugia, C. Evans and M. Tegel, *J. Phys. Chem.*, **2006**, A110, 7952 (d) L. J. Farrugia, C. Evans, D. Lentz, M. Roemer, *J. Am. Chem. Soc.*, **2009**, 131, 1251. (e) G. Gervasio, D. Marabello, R. Bianchi and A. Forni, *J. Phys. Chem.*, **2010**, A114, 9368. (f) M. Niskanen, P. Hirva, M. Haukka, *J. Chem. Theory Comput.*, **2009**, 5, 1084.

[4](a) Macchi, P.; Sironi, A. Coord. *Chem. Rev*. **2003**, 238, 383. (b) M. Feliz, R. Llusar, J. Andr es, S. Berski, B. Silvi. *New J. Chem.* **2002**, 26, 844. (c) I. Bytheway, C. S. Griffith, G. A. Koutsantonis, B. W. Skelton, A. H. White, *Eur. J. Inorg. Chem.* **2007**, 3240.

[5] (a) F. E. Hahn, *Angew. Chem., Int. Ed.*, **2006**, 45, 1348. (b) M. Melaimi, M. Soleihavoup and G. Bertrand, *Angew. Chem.,Int. Ed.*, **2010**, 49, 8810. (c) S. Díez-Gonzalez, N. Marion and S. P. Nolan, *Chem. Rev.*, **2009**, 109, 3216. (d) F. A. Glorius, *Top. Organomet. Chem.*, **2007**, 21, 1. (e) O. Kaufhold and F. E. Hahn,. *Angew. Chem., Int. Ed.*, **2008**, 47, 4057.

[6] (a) W. A. Herrmann, *Angew. Chem., Int. Ed.*, **2002**, 41, 1290. (b) F. E. Hahn and M. C. Jahnke, *Angew. Chem., Int. Ed.*, **2008**, 47, 3122.

[7] (a) H. Braunschweig, R. D. Dewhurst, K. Hammond, J. Mies, K. Radacki and A. Vargas, *Science*, **2012**, 336, 1420 (b) H. Braunschweig, A. Damme, R. D. Dewhurst and A. Vargas, *Nat. Chem.*, **2012**, 5, 115. (c) K. Hirano, S. Urban, C. Wang and F. Glorius, *Org.Lett.*, **2009**, 11, 1019. (d) R. Tonner and G. Frenking, *Organometallics*, **2009**, 28, 3901. (e) D. G. Gusev, *Organometallics*, **2009**, 28, 6458. (f) G. Song, Y. Zhang and X. Li, *Organometallics*, **2008**, 27, 1936.

[8] (a) J. C. Y. Lin, R. T. W. Huang, C. S. Lee, A. Bhattacharyya, W. S. Hwang and I. J. B. Lin, *Chem. Rev.*, **2009**, 109, 3561. (b) P. de Fre´mont, N. Marion and S. P. Nolan, *Coord. Chem. Rev.*, **2009**, 253, 862. (c) H. Clavier, K. Grela, A. Kirschning, M. Mauduit and S. P. Nolan, *Angew. Chem., Int. Ed.*, **2007**, 46, 6786.

[9] W. Scherer, M. Tafipolsky and K. Ofele, *Inorg. Chim. Acta.*, **2008**, 361, 513.

[10] M. Tafipolsky, W. Scherer, K. Ofele, G. Artus, B. Pedersen, W. A. Herrmann, G. S. McGrady, *J. Am. Chem. Soc.* **2002**, 124, 5865.

[11] J. A. Cabeza, Juan F. Van der Maelen and S. García-Granda, *organometallics*, **2009**, 28, 3666.

[12] J. A. Cabeza, M. Damonte and P. García-A lvarez , *Organometallics*, **2011**, 30, 2371.

[13] M. J. Frisch, G. W. Trucks, H. B. Schlegel, G. E. Scuseria, M. A. Robb, J. R. Cheeseman, G. Scalmani, V. Barone, B. Mennucci, G. A. Petersson, H.

Nakatsuji, M. 182 Caricato, X. Li, H. P. Hratchian, A. F. Izmaylov, J. Bloino, G. Zheng, J. L. Sonnenberg, M. Hada, M. Ehara, K. Toyota, R. Fukuda, J. Hasegawa, M. Ishida, T. Nakajima, Y. Honda, O. Kitao, H. Nakai, T. Vreven, J. A. Montgomery, J. E. Peralta, F. Ogliaro, M. Bearpark, J. J. Heyd, E. Brothers, K. N. Kudin, V. N. Staroverov, R. Kobayashi, J. Normand, K. Raghavachari, A. Rendell, J. C. Burant, S. S. Iyengar, J. Tomasi, M. Cossi, N. Rega, J. M. Millam, M. Klene, J. E. Knox, J. B. Cross, V. Bakken, C. Adamo, J. Jaramillo, R. Gomperts, R. E. Stratmann, O. Yazyev, A. J. Austin, R. Cammi, C. Pomelli, J. W. Ochterski, R. L. Martin, K. Morokuma, V. G. Zakrzewski, G. A. Voth, P. Salvador, J. J. Dannenberg, S. Dapprich, A. D. Daniels, O. Farkas, J. B. Foresman, J. V. Ortiz, J. Cioslowski, and D. J. Fox, *Gaussian 09, Revision A.02*, Gaussian, Inc., Wallingford CT, **2009**.

[14] C. Adamo and V. Barone, *J. Chem. Phys*., **1999**, 110, 6158.

[15] W. J. Hehre, R. Ditchfield and J. A. Pople, *J. Chem. Phys*., **1972**, 56, 2257.

[16] P. Fuentealba, H. Stoll, L. V. Szentpaly, P. Schwerdtfeger and H. Preuss, *J. Phys. B.*, **1983**, 16, L323.

[17] A. Höllwarth, M. Böhme, S. Dapprich, A. W. Ehlers, A. Gobbi, V. Jonas, K. F. Köhler, R. Stegmann, A. Veldkamp and G. Frenking, *Chem. Phys. Lett.*, **1993**, 208, 237.

[18] S. Huzinaga, M. Klobukowski, *Chem. Phys. Lett*. **1993**, 212, 260.

[19] F. Biegler-König and J. Schönbohm, *AIM2000*, version 2.0, Bürofür Innovative Software, **2002**.

[20]P. Macchi, L. Garlaschelli, S. Martinego, A. Sironi, *J. Am. Chem. Soc.* **1999**, *121*, 10428.

[21] U. Flierler, M. Burzler, D. Leusser, J. Henn, H. Ott, H. Braunschweig, D. Stalke, *Angew. Chem., Int. Ed.* **2008**, *47*, 4321.

[22] (a) J. Overgaard, H. F. Clausen, J. A. Platts, B. B. Iversen, *J. Am. Chem. Soc.* **2008**, *130*, 3834. (b) J. Overgaard, J. A. Platts, B. B. Iversen, *Acta Crystallogr., Sect. B* **2009**, *65*, 715. (c) J. A. Platts , G. J. S.Evans, M. P. Coogan, J. Overgaard, *Inorg. Chem.* **2007**, *46*, 6291. (d) Y. Ortin, N. Lugan, S. Pillet, M. Souhassou, C. Lecomte, K. Costaus, , J.-Y. Saillard, *Inorg. Chem.* **2005**, *44*, 9607.

[23] L. J. Farrugia, C. *C. R.* Evans, *Chim.*, **2005**, *8*, 1566.

[24] Ch. F. Matta , The Quantum Theory of Atoms in Molecules, Wiley-VCH Weinheim, Germany, **2007**.

[25] C. Gatti and D. Lasi, *Faraday Discuss*., **2007**, 135, 55.

[26] G. Gervasio, R. Bianchi and D. Marabello, *Chem. Phys. Lett*., **2005**, 407, 1.

[27] C. Z. Gatti, *Kristallogr*. **2005**, 220, 399.

[28] (a) R. F. W. Bader, M. E. Stephens, *J. Am. Chem. Soc.* **1975**, 97, 7391. (b) X. Fradera, M. A. Austen, R. F. W. Bader, *J. Phys. Chem. A***1999**, 103, 304. (c) E. Matito, M. Sola` *Coord. Chem. ReV.* **2009**, 253, 647.

[29] (a) J. Poater, M. Sola`, M. Duran, X. Fradera, *Theor. Chem. Acta* **2002**, 107, 362. (b) T. Kar, J. G. A´ ngya´n, A. B. Sannigrahi, *J. Phys. Chem.A* **2000**, 104, 9953.

[30] J. F. Van der Maelen , S. García-Granda , J. A. Cabeza, *Computational and Theoretical Chemistry*, 2011, 968, 55.

[31] L. J. Farrugia and H. M. Senn *J. Phys. Chem. A* **2010**, 114, 13418.

[32] Macchi, P.; Donghi, D.; Sironi, A. *J. Am. Chem. Soc.,***2005**, *127*, 16494.

[33] C. Bo, J. P. Sarasa, J. M. Poblet, *J.Phys.Chem.* **1993**, 97, 6362.

[34] A. A. Low, K. L. Kunze, P. J. MacDougall, M. B. Hall, *Inorg. Chem.* **1991**, 30, 1079.

[35] Y. A. Abramov, L. Brammer, W. T. Klooster, R. M. Bullock, *Inorg. Chem.* **1998**, 37, 6317.
[36] A. I. Stash, K. Tanaka, K. Shiozawa, H. Makino, V. G. Tsirelson, *Acta Crystallogr. B* **2005**, 61, 418.
[37] S. Pillet, G. Wu, V. Kulsomphob, B. G. Harvey, R. D. Ernst, P. Coppens, *J. Am. Chem. Soc.* **2003**, 125, 1937.
[38] C.-C. Wang, Y. Wang, H.-J. Liu, K.-J. Lin, L.-K. Chou, K.-S. Chan, *J. Phys. Chem. A* **1997**, 101, 8887.
[39] R. Bianchi, G. Gervasio, D. Marabello, *Acta Crystallogr. B***2001**, 57, 638.
[40] T. S. Koritsanszky, P. Coppens, *Chem. Rev.* **2001**, 101, 1583.
[41] M. Esma¨ıl Alikhani, *Phys.Chem. Chem. Phys*., **2013**, 15, 12602.

الخلاصة

تمت دراسة التاصر الموجود في مركب برديل نايتروجين كاربين الحلقي كاربونايل ثلاثي الروثينيوم العنقودي **$[Ru_3(\mu-H)(\mu-\kappa^3C_2,N-pyCH_2ImMe)(CO)_9]$** باستخدام نظرية الكم للذرات في الجزيئات. تم حساب جميع خصائص التاصر في النقطة الحرجة (bcp) لكل اصرة من اواصر فلز – فلز وفلز- ليكاند والمتمثله بالكثافة الالكترونية $\rho(r)$، قيم لابلاس $\nabla 2\rho(r)$، الطاقة الكلية $G(r)$ للكثافات الالكترونية، الطاقة الحركية $H(r)$ للكثافات الالكترونية و الالبتستي وكذلك قيم عدم تمركز الاصرة δ (A، B) ومقارنتها مع النتائج المستحصلة من الدراسات السابقة للأنظمة الفلزية العضوية. وتمخضت من هذه النتائج اجراء مقارنة لخصائص التبولوجيا للتاصر بين الذرات. ان نتائج التبولوجيا المحسوبة في قلب ثلاثي الروثنيوم العنقودي المتمثل بالجزء (Ru_3H) اثبتت وجود تاصر بين ذرتي روثينيوم Ru2 -Ru1 وكذلك بين ذرتي روثنيوم Ru3–Ru1 وانعدام مثل هذا التاصر بين Ru3–Ru2المرتبطتان بالهايدرايد الجسري بالرغم من وجود قيمة لمعامل عدم التمركز (delocalization index) $\delta(Ru(2)...Ru(3))$ لها. اثبتت الدراسة وجود تفاعل متعدد المراكز من نوع 4C–4e للجزء الخاص بقلب المركب والمتمثل ب Ru_3H. ان معاملات التبولوجيا المحسوبه لاصرتي الروثينيوم والكاربون في ليكاندات البريديل NHC, كانت متشابة ومن نوع اواصرسكما σ. اظهرت معاملات التبولوجيا المحسوبة للاواصر الموجودة بين ذرات اليكاندين (NHC) و(البرديل) وجود عدم تمركز لالكترونات π داخل الحلقة السداسية بالنسبة لليكاند (البرديل) وتقييد في عدم التمركز لإلكترونات π داخل الحلقة الخماسية في ليكاند (NHC) مع وجود بعض الاواصر المزدوجة بين ذرة الكاربين C و ذرات N المجاورة لها.